Proceedings of the ICBBG2025
2025 International conference on Bio-mediated and Bio-inspired Geotechnics
18-20 May, 2025 | Tempe, Arizona, USA
https://doi.org/10.53243/ICBBG2025-136

Evaluation of the Capacity of Deployable Granular Anchors in Sands

Aly Ghanem[1] and Alejandro Martinez[2]

[1]Department of Civil and Environmental Engineering, University of California Davis, 2001 Ghausi Hall, Davis CA, 95616; e-mail: aghanem@ucdavis.edu
[2]Department of Civil and Environmental Engineering, University of California Davis, 2001 Ghausi Hall, Davis CA, 95616; e-mail: amart@ucdavis.edu

ABSTRACT

Soil penetration is a common process in civil infrastructure applications such as in-situ testing or sensor installation for monitoring soils. Challenges arise in sites with limited accessibility or stiff layers due to the inability to mobilize rigs with the reaction mass required to reach desired depths. This research evaluates the feasibility of using bio-inspired probes with deployable granular anchors to generate required reaction forces. The conceptual anchor consists of a flexible membrane filled with a granular material, connected to an air pressure/suction source. Pressure is used to radially deploy the anchor, while suction is applied to increase the granular materials' strength and stiffness during anchorage. This research uses analytical solutions to evaluate the variation of anchor capacity with depth in sands, considering failure of the external soil mass and of the internal granular material as the limiting conditions. Solutions for uplift capacity of circular plate anchors and cavity expansion are used to determine the capacity of the surrounding soil mass and within the anchor. The anchor capacity is the minimum of these two capacities, which is shown to depend on the anchor expansion magnitude, operation, and applied suction. Results show that the granular anchor can mobilize the soil resistance or a significant portion of it, depending on the anchor operation, making it a feasible solution for deploying temporary anchors in-situ.

INTRODUCTION

Characterizing sites with limited accessibility, such as forested areas, post-hazard locations, or outer space bodies, presents challenges due to the difficulties associated with mobilizing rigs capable of generating the required reaction mass. To address this, researchers have proposed using bio-inspired probes with an expandable section behind the tip acting as a temporary anchor. The design mimics the burrowing mechanism of organisms such as razor clams and earthworms, which anchor parts of their bodies to the surrounding soil to facilitate forward movement. Martinez et al. (2019) and (2022) provided a summary of these organisms' locomotion mechanisms, typical dimensions, and depths at which they typically exist. More information is available in the original work of Dorgan (2018). In these bio-inspired probes, the expanded anchor increases the radial pressure, improving frictional capacity along the shaft, and forms a ring-shaped area at the top that mobilizes a bearing component. The development of such probes has the potential to facilitate site investigation and sensor installation with lightweight equipment. Martinez et al. (2024) presents a summary of relevant research on bio-inspired probes.

Previous studies have explored prototypes utilizing this bio-inspired mechanism. Martinez et al. (2019) used cavity expansion analysis to determine anchor dimensions required to achieve

self-burrowing, and found that L/D ratios between 2 and 4.5 are sufficient for different deposits in both sands and clays. Chen et al. (2022) used 3D Discrete Element Modeling (DEM) to study stress alterations around a bio-inspired probe, showing that anchor expansion reduces effective stresses at the tip due to arching, tip advancement remobilizes the tip resistance, and simultaneous tip advancement and anchorage reduces radial stresses generated around the anchor. These and other similar studies only considered external soil failure in estimating anchor capacity, assuming the anchor won't fail internally. This assumption possesses practical challenges as the anchor needs to be flexible enough to initially expand and stiff enough to resist the uplift forces. Borela et al. (2020) manufactured a probe with an air-pressurized anchor, and monitored the soil's deformations during its operation using X-ray tomography. Their results showed that the anchor backslid due to the tip resistance exceeding the anchor's capacity. He et al. (2024) developed a dual-anchor prototype using a similar anchor design, which failed to borrow downwards due to the stress gradient. Similarly, Tao et al. (2020) highlighted that additional features are required to overcome the natural stress gradient of soil and allow downward burrowing.

These findings highlighted two key necessities for prototypes of this type: (1) an anchor that is rigid enough to generate sufficient reaction forces to overcome tip resistance, and (2) a robust actuator to efficiently transfer the generated capacity from the anchor to the tip without excessive deformation. To address the first challenge, this study proposes filling the anchor with a granular material, a technique widely used in soft robotics due to the phase changing nature of these materials (i.e., from solid-like to liquid-like and vice versa). This research investigates the efficiency of the proposed granular anchor by comparing the external and internal capacities across different anchor operation parameters for specific sand deposit.

GRANULAR MATERIALS FOR ROBOTICS

Granular materials exhibit clear phase changing characteristics. This is a result of the geometrical disorder of its particles, lacking of particle bonding, and boundary conditions. This leads to the development of different and continuously varying physical properties depending on the applied boundary conditions, ranging from solid-like to liquid-like behaviors. This dynamic nature makes granular materials favorable in soft robotic applications where altering the stiffness is required.

Granular grippers have been proposed, where a flexible membrane is filled with a granular material and connected to a suction source (Brown et al. 2010). The material is initially deformable to allow the gripper to conform around an object (i.e., liquid-like behavior), then suction is applied to jam the material and firmly grip the object (i.e., solid-like behavior). The same principle is used in locomotion, where a robot was supplemented with jamming paws to increase compliance and friction against the walls to vertically ascend it (Hauser et al. 2018). Our study proposes using the same principle, where the bio-inspired probe's anchor is initially deformable for deployment and then rigid during anchorage.

PROPOSED ANCHOR DESIGN

A conceptual design of the probe with an integrated anchor is proposed to estimate the anchoring capacity. The prototype shown in Figure 1a features a probe with an expandable shaft section behind its tip which is filled with a granular material. The shaft is expanded to form a temporary anchor, with the granular material conforming to the expanded shape. After expansion, suction is

applied internally to jam the granular material by increasing the confining stress which increases its stiffness and strength, allowing for mobilization of higher anchor capacities.

The anchor has an initial diameter equal to the probe's diameter (D_p), and a diameter (D_a) after expansion. The relation between both diameters is described by the expansion magnitude (EM), where $EM = D_a/D_p - 1$. The length of the anchor (L_a) is defined using a normalized quantity L_a/D_p. The granular material's strength is modeled using the Mohr-Colomb's failure criterion, assuming a perfectly frictional material having a friction angle (ϕ_{int}). During the anchoring process, the anchor is expected to experience enough deformations such that the granular material is at the critical state; therefore, ϕ_{int} is assumed to be the critical state value. The anchor is expanded by application of pressure, while application of a suction of magnitude P_s enables jamming. The probe considered in this study has a D_p of 4.4 cm, corresponding to a CPT probe with an area of 15 cm², and features a granular anchor positioned behind the tip with an L_a/D_p of 4 filled with a granular material with ϕ_{int} of 35°. The study investigates the effect of the anchor operation on its capacity by varying EM, P_s, and the control of anchor suction during pullout.

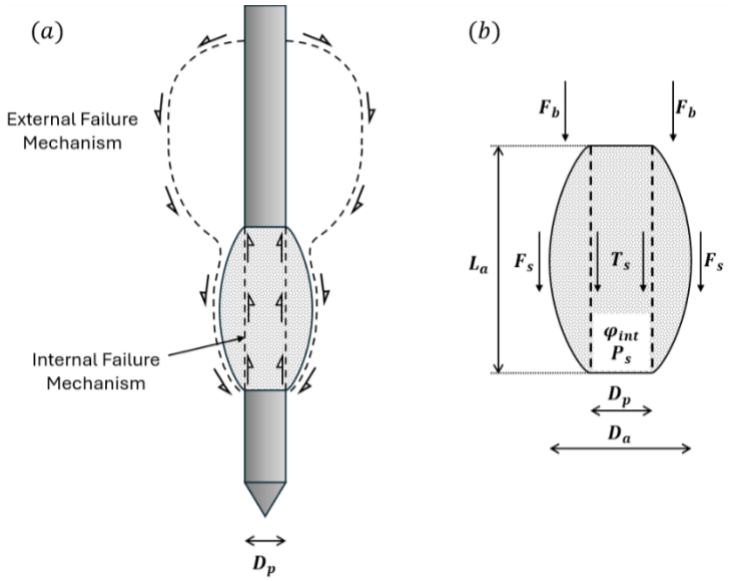

Figure 1. (a) Proposed prototype, (b) anchor properties and forces contributing to its capacity

FRAMEWORK FOR ANCHOR CAPACITY EVALUATION

The two possible failure mechanisms during pullout loading are external failure of the surrounding soil and internal failure of the granular material within the anchor. The external capacity is calculated as the sum of bearing at the top and friction along its shaft, while the internal capacity is estimated from the shear strength of an assumed cylindrical failure surface. The ultimate capacity of the anchor is taken as the minimum of the external and internal capacities.

Figure 1b shows the different components contributing to the anchor capacity during axial loading. As depicted in the figure, the external and internal capacities can be expressed as shown in Equations 1 and 2 in Table 1, where F_b is the bearing force at the top of the anchor, F_s is the friction force along the anchor's side, and T_s is the shear capacity of the internal failure which is assumed to be cylindrical in shape. Each component is calculated according to Equations 3, 4, and 5 in Table 1, where q_b is the bearing capacity at the top of the anchor, q_s is the skin friction at the

mid-height of the anchor, and τ_s is the shear strength of the internal failure surface, while A_b is the ring-shaped bearing area, A_s is the shaft area, and A_{int} is the area of the internal cylindrical failure surface. The areas are calculated using Equations 6 to 8.

Table 1: Equations for determination of the granular anchor capacity.

$Q_{ext} = F_b + F_s$	(1)	$Q_{int} = T_s$	(2)
$F_b = q_b * A_b$	(3)	$F_s = q_s * A_s$	(4)
$T_s = \tau_s * A_{int}$	(5)	$A_b = {}^{\pi}/_{4}\left({D_a}^2 - {D_p}^2\right)$	(6)
$A_s = \pi * D_a * L_a$	(7)	$A_{int} = \pi * D_p * L_a$	(8)
$q_b = N_q * {\sigma_{vo}}'$	(9)	$q_s = {}^{{P_L}'}/_{R} * \tan\delta$	(10)
$\tau_s = \left({}^{{P_L}'}/_{R} + P_s\right)\tan\varphi_{int}$	(11)		

The bearing capacity at the top of the anchor is considered analogous to the uplift capacity of a circular plate anchor, while the shaft friction is considered analogous to friction capacity of a pile. The internal mechanism was considered as soil shearing along an assumed cylindrical area. Since both external and internal materials are coarse-grained, effective stress analyses are used. The unit resistances are therefore using Equations 9 to 11, where N_q is the dimensionless breakout factor calculated using plate anchor uplift solutions, σ_{vo}' is the initial vertical effective stress at the top of the anchor, P_L' is the effective limiting radial pressure at the mid-height of the anchor after expansion calculated using cavity expansion theory, and δ is the interface friction angle between the anchor and soil, assumed to be 2/3 of the external soil's ϕ_{cs}.

The reduction factor "*R*" in Equations 10 and 11 accounts for the expected reduction in radial pressure during pullout loading when the anchor diameter is kept constant, as observed by Chen et al. (2022) in DEM simulations. When simulating a probe with the same geometry assumed for this study, limiting pressures dropped by a factor of about 2. However, no reduction would occur if the radial pressure at the end of expansion is maintained by continuous expansion of the anchor during pullout (Chen et al. 2024). Therefore, the effect of the reduction factor on the anchor capacity is evaluated by considering two limiting conditions: (1) initial expansion magnitude is maintained leading to $R = 2$, and (2) constant pressure is maintained leading to $R = 1$. For partially maintained radial pressure, an intermediate R value of 1.5 will be evaluated. Since the R value of 2 is based on DEM observations, it should be validated using experiments in the future.

Modeling of the Soil Deposit. The uplift capacity of plate anchors has been thoroughly investigated and was therefore implemented in this study. To calculate external shaft friction and internal capacity, the increase in normal radial stress due to anchor expansion needs to be evaluated. This was done using the theory of cavity expansion, where the radial stresses after expansion are assumed to be equal to the limiting radial pressures resulting from expanding a cylindrical cavity. Limiting pressures were calculated using the ASCEND code (Applications for Spherical and Cylindrical Cavity Expansion in Nonlinearly Deforming Geomaterials) developed by Jaeger, which incorporates the constitutive model MIT-S1 (Pestana and Whittle, 1999) to simulate soil behavior. Model calibration parameters are available for Toyoura Sand and are summarized in Martinez et al. (2019).

The ASCEND program calculates the limiting pressure at different depths as a function of critical state friction angle and state parameter (ψ), while published solutions for the plate anchor uplift capacity are presented as functions of the peak friction angle. The peak friction angle's dependency on the effective stress and critical state friction angle was therefore considered using

the Bolton (1986) framework. The relative density required for using Bolton's equations was related to the ψ using maximum and minimum void ratios and critical state line parameters of Toyoura sand. Maximum and minimum void ratios are found by Verdugo and Ishihara (1996) to be equal to 0.977 and 0.597, which are used for this study to calculate the deposit's void ratio for an assumed relative density of 60%. Verdugo and Ishihara (1996) showed that the critical state void ratio at p' = 100 kPa ($e_{cs,100}$) is equal to 0.913, and Bellotti et al. (1997) mentioned that Verdugo (1989) found the slope of the critical state line to be equal to 0.021. The slope of the recompression line (κ) was taken as 0.005 (Martinez et al. 2019). These values were used to calculate the critical state void ratio, and accordingly the ψ at any depth as a function of the mean effective stress.

Uplift Capacity. The uplift capacity of plate anchors was estimated by considering developed analytical solutions (Meyerhof and Adams, 1963; Tagaya, 1988). Their analyses distinctly considered shallow and deep failure. Solutions from different studies were found to vary, and the method used in this study was that which provided anchor capacities close to those reported by Chen et al. (2022) based on DEM simulations. This criterion was used as an attempt to account for the expected differences between the failure mechanism of circular plate anchors and the cylindrical-shaped anchor. The comparison showed that the equations reported by Tagaya (1988) provided close estimates of the uplift forces.

Limiting Pressure. ASCEND calculates limiting pressures at discrete combinations of effective vertical stress (σ_v') and ψ. Since ψ changes with depth, limiting pressures had to be defined in a continuous fashion. Results obtained from the program were therefore plotted against effective stress for different ψ. A power function was found to best represent the relation, which agreed with fundamental understanding of the process as it estimates a zero-value at zero effective stress as shown in Figure 2. Fitted equations were used to determine P_L' at any combination of ψ and σ'_v.

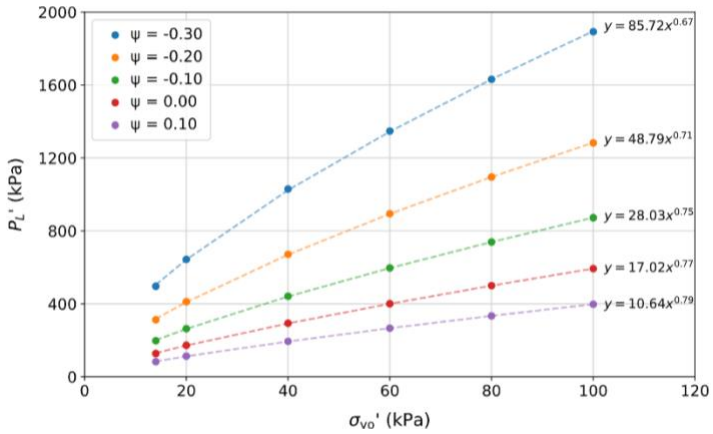

Figure 2. Effective limiting pressure at different effective vertical stresses and state parameters

RESULTS

A parametric study was conducted to evaluate the effect of different anchor operations. Considered variables for this study were the expansion magnitude (*EM*), the reduction in radial pressure during anchoring (*R*), and the applied suction pressure (P_s). Since the external and internal

capacities depend on the initial effective stress, results are presented as a function of the depth to the top of the anchor (H_{top}) and the normalized depth (H_{top}/D_p).

The internal and external capacities are plot versus depth in Figures 3, 4, and 5. It was observed that the capacity at shallow depths is controlled by the external capacity (i.e., $Q_{ext} < Q_{int}$) and transitions to being controlled by the internal capacity (i.e., $Q_{ext} > Q_{int}$) at a certain depth. Such transition depth is presented using a green dot. When studying the effect of a certain parameter, all other parameters are assigned constant values equal to those of an assumed reference condition which are $EM = 0.5$, $R = 2$, and $P_s = 90$ kPa (vacuum).

Effect of Expansion Magnitude (EM). Increasing *EM* only increases the external capacity as it increases the shaft and bearing areas, as shown in Figure 3. The internal capacity is not affected since it is assumed that the limiting pressure is fully mobilized for all considered *EM* values and the internal failure area (i.e., A_{int}) does not depend on *EM*. Results show that the transition depth decreases as *EM* increases, indicating internal anchor failure at shallower depths as the *EM* value increases.

Effect of Reduction Factor (R). The reduction factor affects the external and internal capacities through changing the limiting pressures, as shown in Figure 4. The effect of decreasing *R* is more pronounced on the internal capacity as Q_b which is independent of *R* contributes to the external capacity. Therefore, the transition depth increases as *R* is decreased. This is the case if the external capacity controls (i.e., $Q_{ext} > Q_{int}$) at shallow depths, which is true if suction is applied to the anchor.

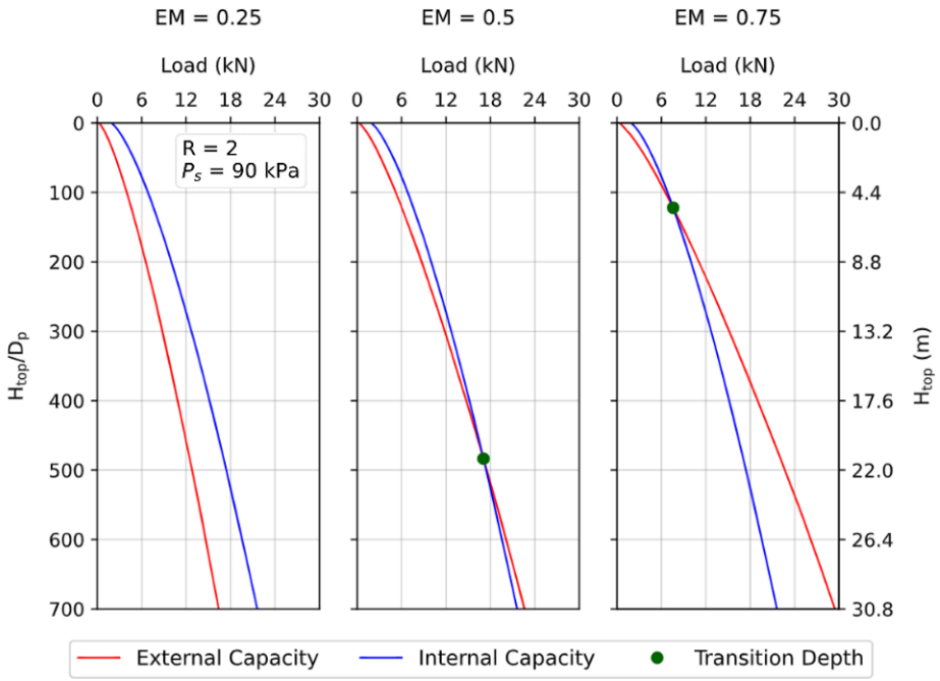

Figure 3. Effect of changing expansion magnitude on the capacity profiles

Effect of Suction Pressure (P_s). Suction pressure increases the internal capacity by a constant value (ΔQ_{int}) at all depth due to the uniform increase in confining pressure applied to the granular material within the anchor, as shown in Figure 5. The increase in suction drives the transition depth deeper, which indicates that the anchor is able to mobilize the external soil's strength along a

greater depth. The rate at which the transition depth increases depends on the relative rates of increase of the external and internal capacities.

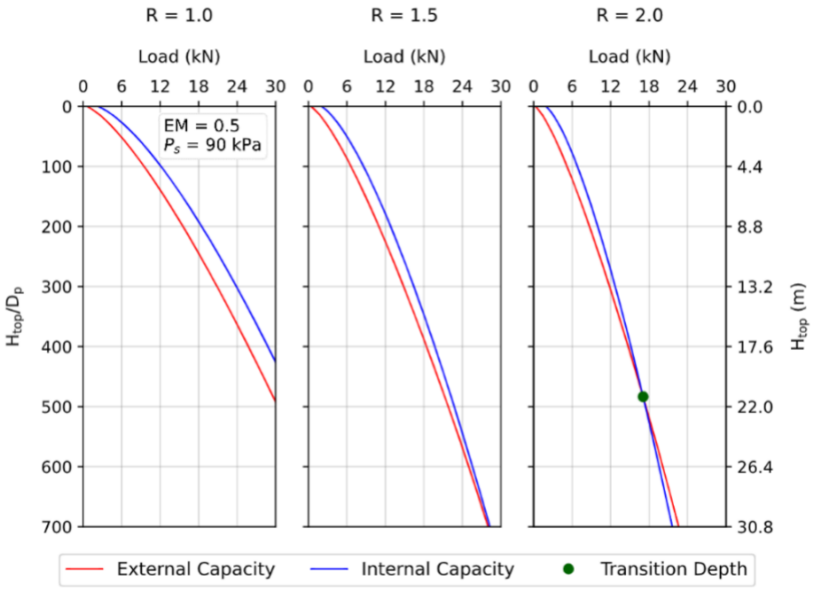

Figure 4. Effect of changing the reduction factor on the capacity profiles

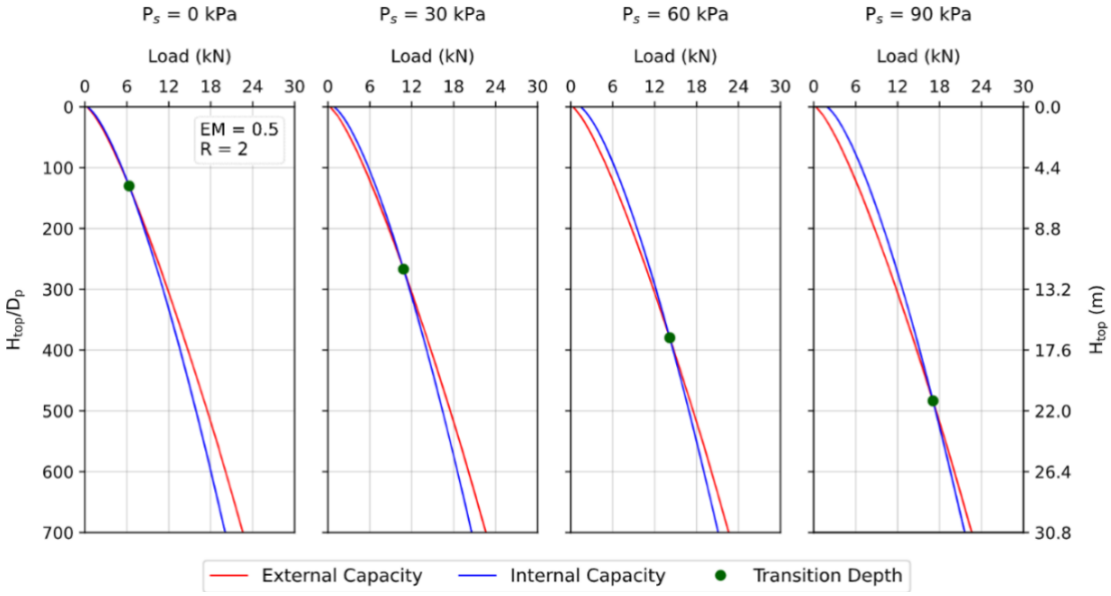

Figure 5. Effect of changing suction pressure on the capacity profiles

DISCUSSION

Contribution to external capacity. Understanding how different factors contribute to Q_{ext} is essential for designing and operating the anchor efficiently. The external capacity is the sum of the Q_s and Q_b, and variables that affect them alter the relative contribution to the anchor's capacity. This is captured by plotting the ratio Q_b/Q_{ext} versus each varied parameter at three different depths in Figure 6. A dashed line is drawn at a ratio of 0.5, such that the higher values represent a greater Q_b contribution and lower values indicate a greater Q_s contribution. The results indicate that the

contribution of Q_s is greater in all cases. This is because A_s is much bigger than A_b. Despite this, the contribution of Q_b increases with depth. This implies that the rate of increase in the bearing pressure with depth is higher than the rate increase in the limit pressure acting on the anchor's shaft. Increasing EM increases A_b at a higher rate (i.e., by D_a^2) than it does for the A_s (i.e., by D_a), and therefore increases the contribution of Q_b. Decreasing the R factor increases the shaft friction, which leads to a lower Q_b contribution. The suction pressure only affects the internal capacity, and therefore does not affect the relative contribution to the external capacity.

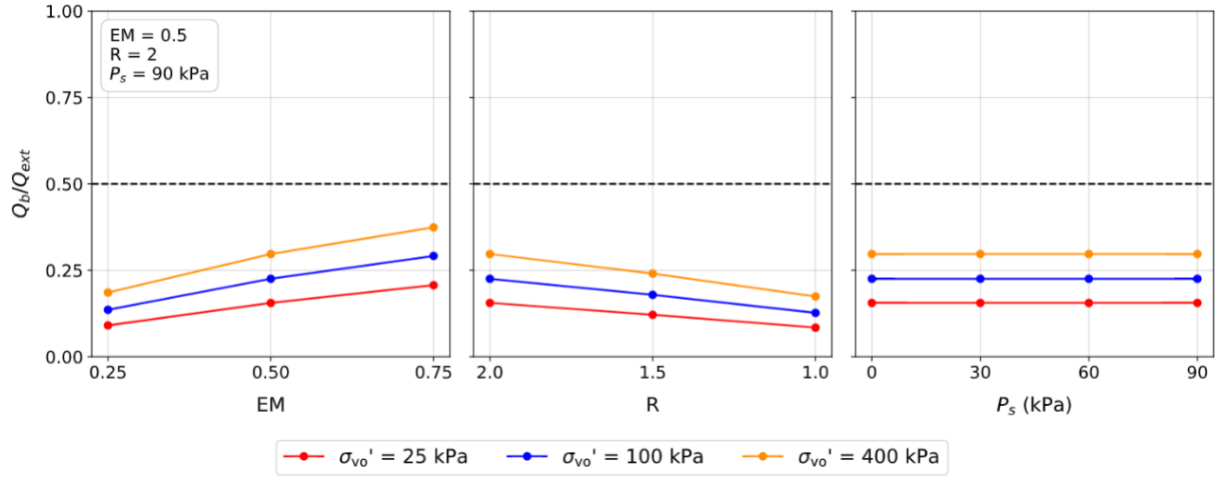

Figure 6. Effect of each operation parameter on the bearing contribution to the external capacity

Comparison of external and internal capacities. The relative magnitude between Q_{ext} and Q_{int} indicates which type of failure governs at any given depth. Figure 7 presents the ratio Q_{ext}/Q_{int} versus each variable at different depths. The plotted line at a ratio of 1.0 indicates the $Q_{ext} = Q_{int}$ condition corresponding to the transition depth discussed earlier. Values lower than 1.0 indicate external soil failure indicating that the surrounding soil is fully mobilized, while value greater than 1.0 indicate internal failure.

The effect on the ultimate capacity must be considered when evaluating the ratio between external and internal capacity, as the ratio could change while the overall anchor capacity remains constant. If a variable increases both internal and external capacity, such as R, the anchor capacity continuously increases. In contrast, EM only affects Q_{ext} while P_s only affects Q_{int}. For such cases, the anchor capacity improvement depends on how the ratio Q_{ext}/Q_{int} changes. The anchor capacity improves if the capacity of the governing failure mechanism increases, which is described by the lines getting closer to 1.0. Otherwise, the bigger capacity increases without affecting the anchor capacity because the latter is controlled by the minimum of Q_{ext} and Q_{int}. For clarity, changes that lead to anchor capacity improvement are plotted as solid lines while those that do not affect it are plotted as dashed lines.

The ratio Q_{ext}/Q_{int} increases with depth for all tested conditions, although the internal friction angle is bigger than the external interface friction angle. This implies that the increase in Q_b with depth offsets the relative increase in Q_{int}. Increasing EM increases Q_{ext}/Q_{int} as it only increases Q_{ext}. At each depth, there is an EM value beyond which no improvement in the anchor capacity occurs because Q_{ext} continues to increase beyond the point where internal failure governs the anchor's performance. Since Q_{ext}/Q_{int} increases with depth, the EM value at which no improvement occurs becomes smaller. This implies that the EM needed to fully mobilize the

anchor's internal capacity decreases as the depth is increased. The effect of increasing depth becomes more pronounced as EM increases and R decreases, since EM increases the Q_b contribution while R decreases it. Although P_s does not affect Q_b, the effect of depth becomes higher as P_s increases.

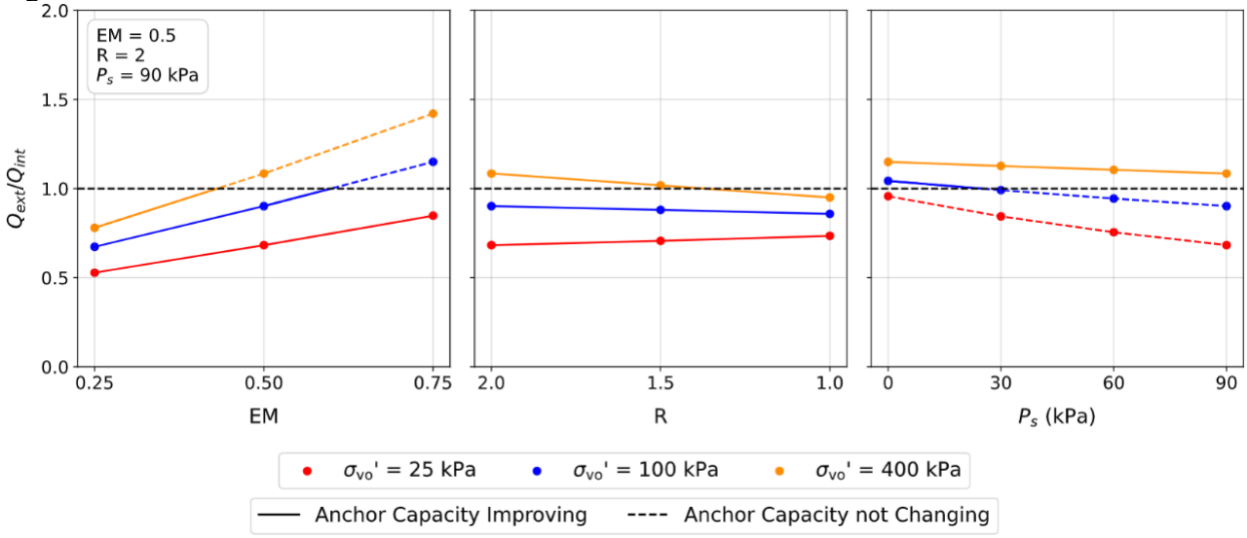

Figure 7. Relation between external and internal capacities at different operation conditions.

Maintaining a lower reduction factor improves the anchor capacity, as it increases Q_{int} and the Q_s component of Q_{ext}. Although the increase in Q_{int} is always bigger than that of Q_s, the trend of Q_{ext}/Q_{int} with R is not always a decreasing one. This is because at shallow depths, P_s is greater relative to the limiting pressure, making the increase in external capacity bigger than that of the internal one. However, this trend changes if no suction is applied. As P_s increases, Q_{int} increases and Q_{ext}/Q_{int} decreases. Increasing P_s beyond a given point does increase the anchor capacity. At shallow depths, small P_s magnitudes are sufficient to mobilize the external soil's capacity, while greater magnitudes are required at greater depth to transition an external failure. Considering that the theoretical limit of suction is 100 kPa, this might not be achievable past a certain depth.

CONCLUSIONS

This research investigates the feasibility of a proposed bio-inspired probe with a deployable anchor that is filled with a granular material which enables it to expand during deployment and maintain its shape during anchorage. An anchor configuration and a representative sandy deposit were considered, and the effects of changing the anchor operation parameters, including the anchor diameter, applied suction, and control strategy, are investigated. This investigation uses limit equilibrium and cavity expansion solutions to estimate the different anchor capacity components.

Anchor operation plays an important role in its capacity. Maintaining a low reduction factor is always beneficial to the overall anchor capacity as it increases both external and internal capacities. However, increasing the expansion magnitude or applied suction only increases one of the two capacities. Therefore, whether or not they improve the overall anchor capacity depends on the ratio of external to internal capacity. If the governing failure mechanism's capacity is improved, so is the anchor capacity. Since both external and internal capacities are affected by the anchor operation, the process needs to be optimized to increase its efficiency. The results show that using

a granular material inside the anchor allows for mobilization of the external soil's full strength or a significant portion of it, which can be used to generate the reaction needed to advance the tip of the probe forward.

ACKNOWLEDGEMENTS

This material is based upon work supported by the National Science Foundation (NSF) under Award No. 1942369 and the Engineering Research Center Program under NSF Cooperative Agreement No. EEC–1449501. Any opinions, findings, and conclusions or recommendations expressed in this material are those of the author(s) and do not necessarily reflect those of the NSF.

REFERENCES

Bellotti, R., J. Benoît, C. Fretti, and M. Jamiolkowski. 1997. "Stiffness of Toyoura Sand from Dilatometer Tests." *J. Geotech. Geoenviron. Eng.*, 123 (9): 836–846.

Bolton, M. D. 1986. "The strength and dilatancy of sands." *Géotechnique*, 36 (1): 65–78.

Borela, R., J. D. Frost, G. Viggiani, and F. Anselmucci. 2021. "Earthworm-inspired robotic locomotion in sand: an experimental study using x-ray tomography." *Géotechnique Letters*, 11 (1): 1–22.

Brown, E., N. Rodenberg, et al. 2010. "Universal robotic gripper based on the jamming of granular material." *Proc. Natl. Acad. Sci. U.S.A.*, 107 (44): 18809–18814.

Chen, Y., A. Martinez, and J. DeJong. 2022. "DEM study of the alteration of the stress state in granular media around a bio-inspired probe." *Can. Geotech. J.*, 59 (10): 1691–1711.

Chen, Y., N. Zhang, R. Fuentes, and A. Martinez. 2024. "A numerical study on the multi-cycle self-burrowing of a dual-anchor probe in shallow coarse-grained soils of varying density." Acta Geotech., 19 (3): 1231–1250.

Dorgan, K. M. 2018. "Kinematics of burrowing by peristalsis in granular sands." *Journal of Experimental Biology*, jeb.167759.

Hauser, S., M. Mutlu, F. Freundler, and A. Ijspeert. 2018. "Stiffness Variability in Jamming of Compliant Granules and a Case Study Application in Climbing Vertical Shafts." *2018 IEEE International Conference on Robotics and Automation (ICRA)*, 1559–1566.

He, J., H. Wang, X. Huang, and F. Yan. 2024. "Experimental study on self-burrowing dual anchor soft probe." *Biogeotechnics*, 2 (3): 100086.

Martinez, A., Dejong, J., et al. (2022). Bio-inspired geotechnical engineering: Principles, current work, opportunities and challenges. Géotechnique, 72(8), 687–705.

Martinez, A., Y. Chen, and R. Anilkumar. 2024. "PLENARY LECTURE - Bio-inspired site characterization - towards soundings with lightweight equipment." *7th International Conference on Geotechnical and Geophysical Site Characterization*.

Martinez, A., J. T. DeJong, R. A. Jaeger, and A. Khosravi. 2019. "Evaluation of self-penetration potential of a bio-inspired site characterization probe by cavity expansion analysis." *Can. Geotech. J.*, 57 (5): 706–716.

Meyerhof, G. G., and J. I. Adams. 1968. "The Ultimate Uplift Capacity of Foundations." *Can. Geotech. J.*, 5 (4): 225–244.

Pestana, J. M., and A. J. Whittle. 1999. "Formulation of a unified constitutive model for clays and sands." *Int. J. Numer. Anal. Meth. Geomech.*, 23 (12): 1215–1243.

Tagaya, K., R. F. Scott, and H. Aboshi. 1988. "Pullout Resistance of Buried Anchor in Sand."

Soils and Foundations, 28 (3): 114–130.
Tao, J. (Julian), S. Huang, and Y. Tang. 2020. “SBOR: a minimalistic soft self-burrowing-out robot inspired by razor clams.” *Bioinspir. Biomim.*, 15 (5): 055003.
Verdugo, R., and K. Ishihara. 1996. “The Steady State of Sandy Soils.” *Soils and Foundations*, 36 (2): 81–91. https://doi.org/10.3208/sandf.36.2_81.